

Spin transfer precessional dynamics in $\text{Co}_{60}\text{Fe}_{20}\text{B}_{20}$ nanocontacts

W. H. Rippard,^{a)} M. R. Pufall, M. L. Schneider, K. Garello, and S. E. Russek
Electromagnetics Division, National Institute of Standards and Technology, Boulder, Colorado 80305, USA

(Received 6 June 2007; accepted 3 December 2007; published online 13 March 2008)

We report on the precessional dynamics in spin transfer oscillators having $\text{Co}_{60}\text{Fe}_{20}\text{B}_{20}$ free layers as a function of annealing time at 225 °C. Repeated annealing reduces the critical current I_c by roughly a factor of 3 and increases the tunability of the oscillation frequency with current df/dI . The decrease in I_c correlates with an increasing giant magnetoresistance (GMR) during the first 3 h of annealing. For longer times, df/dI continues to increase, although the GMR does not. The variations in the macroscopic $\text{Co}_{60}\text{Fe}_{20}\text{B}_{20}$ magnetization parameters and contact dimensions with annealing are not sufficient to account for the later changes. © 2008 American Institute of Physics.

[DOI: [10.1063/1.2838490](https://doi.org/10.1063/1.2838490)]

INTRODUCTION

The spin transfer effect is known to give rise to microwave dynamics in a variety of magnetic nanostructures and magnetic materials. Material systems have included Co, Fe, Ni/Fe, Ni/Fe/Cu alloys, Co/Fe based alloys, and CoFeB alloys.^{1–5} In CoFeB tunnel junction structures, temperature annealing has been shown to be particularly important in optimizing device characteristics, such as the tunneling magnetoresistance.⁶ Here, we show that the temperature annealing of all-metallic spin transfer nanoscale oscillators (STNOs) containing amorphous CoFeB free layers leads to significantly reduced critical currents as well as to increased tunability of the oscillation frequency with current. Over the first three anneals, the spectral output properties of the oscillators with temperature annealing are consistent with changes in the giant magnetoresistance (GMR) of the structure, although the later changes are not. Although $\text{Co}_{60}\text{Fe}_{20}\text{B}_{20}$ has a larger saturation magnetization and a damping parameter and an exchange stiffness similar to that of $\text{Ni}_{80}\text{Fe}_{20}$, the annealing process yields a lower value of the critical current density for the $\text{Co}_{60}\text{Fe}_{20}\text{B}_{20}$ structures, suggesting a method for reducing the critical currents in spin transfer based devices.

EXPERIMENT

The devices discussed here consist of a nominally 50 nm diameter electrical contact made to the top of a continuous $10 \times 20 \mu\text{m}^2$ spin-valve mesa.⁴ The spin valve comprises Ta (3 nm)/Cu (15 nm)/ $\text{Co}_{90}\text{Fe}_{10}$ (20 nm)/Cu (4 nm)/ $\text{Co}_{60}\text{Fe}_{20}\text{B}_{20}$ (5 nm)/Cu(3 nm)/Ta (3 nm). In this structure, precessional motion is induced in the CoFeB layer, and the CoFe layer acts as the “fixed” layer due to its larger thickness and saturation magnetization. The devices are dc current biased so that the precessional motion of the free layer induces a microwave voltage across the device through the GMR effect, which is measured with a spectrum analyzer. All measurements discussed here were performed at room temperature, and all anneals were done at 225 °C in

increments of 60 min in an applied field $\mu_0 H_{\text{anneal}} = 0.1$ T. In our nanocontact geometry, the magnetic material around the contact is protected from exposure to atmosphere by the Ta capping layer throughout the fabrication process and afterwards. The magnetic material which is the vicinity of the contact is further protected from atmosphere from the cross-linked polymethylmethacrylate which forms the insulating barrier in the device structure. These layers act to prevent the formation of magnetic oxides and to prevent the possibility of the annealing either oxidizing the structure or changing local oxidation states within it. The data shown here are for a single device upon repeated annealing, but the qualitative features discussed have been measured in tens of devices in several different applied field geometries.

RESULTS AND DISCUSSION

The spectral output of the STNO devices, i.e., frequency, power output, linewidth, and tunability of frequency with current, varies significantly upon successive annealing, as do the device critical current and GMR value. Figure 1(a) shows the precessional frequencies as a function of dc current for $\mu_0 H_{\text{app}} = 0.85$ T applied at angle $\theta_H = 80^\circ$ out of the film plane for cumulative anneal times up to 6 h. The corresponding oscillation linewidth [full width at half maximum FWHM] and output power (integrated area under the spectral peak) are shown in Figs. 1(b) and 1(c), respectively.

As seen in Fig. 1(a), the annealing process results in an increase in the variation of the oscillation frequency with current df/dI from 0.5 to 3.25 GHz/mA after 6 h of annealing, roughly six times that of the as-prepared sample [see also Fig. 2(a)]. In conjunction, the critical current I_c , determined by the lowest current at which precessional dynamics are measured, is reduced from 6.75 to 2.25 mA after several anneal cycles [see also Fig. 2(b)]. For comparison, similar devices having NiFe as the free layer typically have critical currents of 4–5 mA and frequency tunabilities of roughly 0.5–1 GHz/mA.⁷ Hence, annealing results in comparatively reduced values for I_c and increased values for df/dI in CoFeB structures compared to similar NiFe based devices.

^{a)}Electronic mail: rippard@boulder.nist.gov.

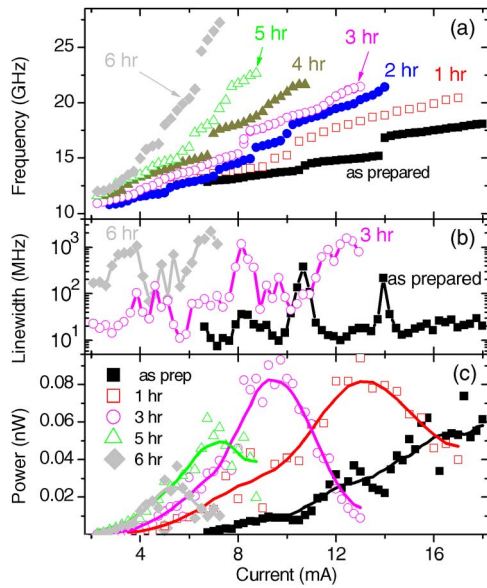


FIG. 1. (Color online) (a) Frequency vs current bias for cumulative anneal times ranging from 0 to 6 h, as labeled. (b) Representative data showing the oscillator linewidth (FWHM) vs current bias for several different anneal times, only three times are shown for clarity. (c) Representative data showing the output power vs current bias for several different anneal times. The solid lines are spline fits to the data and are added only for visual clarity. The symbols in all parts correspond to the same cumulative anneal times.

We note that transmission electron microscopy studies have verified that the CoFeB layer remains amorphous throughout the annealing process.

There is also a change in the variation of frequency with applied field $df/d\mu_0 H$ during the temperature annealing process. However, its value is more difficult to quantify. The locations of the discontinuous jumps of frequency with current are sensitive functions of applied field,⁷ and there is only a relatively small range of accessible fields over which the dynamics can be measured ($\mu_0 H_{\text{app}} = 0.6 - 1.1$ T). Experimentally, this results in values for $df/d\mu_0 H$ ranging from 10 to 35 GHz/T, depending on the particular choice for the applied bias current.

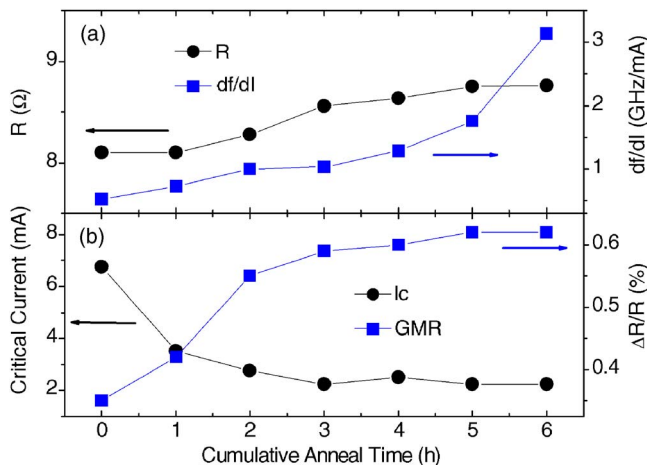


FIG. 2. (Color online) (a) Zero-bias device resistance and df/dI as functions of the cumulative anneal time. (b) Critical current and the GMR value as functions of the cumulative anneal time. The GMR values were determined from CIP measurements of a similarly prepared spin-valve structure.

For this geometry, the oscillation linewidth generally varies significantly as a function of current.⁷ As seen in Fig. 1(b), the linewidth also generally broadens with anneal time. In addition, the annealing process also changes the device output power [Fig. 1(c)]. Upon initial anneal, the maximum output power increases. In this case, it is possible that increased powers from the as-prepared device could be obtained for larger currents since the device dynamics have not ceased at $I = 18$ mA. However, we have explicitly measured several other devices in which the precessional dynamics turn off at the highest applied currents and still found an increase in output power upon annealing. For the device shown here, all of the precessional dynamics have turned off at the highest current levels shown, except for the initial anneal and the as-prepared states. For a cumulative anneal time of up to 3 h, the maximum power remains relatively constant and then decreases upon further annealing. As we discuss below, this behavior is consistent with an initial increase in the GMR of the device with temperature annealing and a reduction in the current being passed through the device, as the device output power scales as $I^2 \Delta R$, where ΔR is the change in resistance associated with the magnetic excitation. As discussed elsewhere, the currents applied to the devices result in Joule heating of a few tens of degrees celsius.^{8,9} Hence, heating effects are not sufficient to result in changes of the device GMR as a function of current bias.

The decrease in I_c correlates with an increase in the GMR value of the CoFe/CoFeB spin valve with annealing. Current-in-plane (CIP) GMR measurements of a similarly prepared spin valve are shown as a function of the cumulative anneal time in Fig. 2(b). During the first 3 h of annealing, the GMR increases^{10,11} from 0.3% to roughly 0.6% and then remains relatively constant upon further annealing.¹² During these initial anneals, the critical current in the nanocontact is reduced by a factor of 3 from 6.75 to 2.25 mA and then remains relatively constant during subsequent anneals. The correlation between the changes in the GMR and the values of the critical current suggests that changes in the spin-dependent transport in the device occur during the initial anneals and are responsible for an increased spin torque efficiency and the reduced values of I_c , in accordance with Ref. 13.

The f vs I curves do not follow a universal dependence since normalizing the bias current by the critical current for a given data set does not give agreement among the precessional frequencies for the various anneal times. This suggests that the precessional trajectories themselves are changing. The closest agreement occurs among the first three anneals and is significantly worse for longer anneal times. This can be seen in Fig. 1(a). For anneal times longer than 3 h, the critical current does not change. Hence, normalizing the bias current by I_c will not change the relative frequency differences for these data. Some of the initial increase in df/dI may result from the decreased critical currents since, for a given absolute current, the normalized bias current I/I_c is increasing during the first three anneals. However, during these first anneals, the critical current changes by a factor of 3, whereas df/dI varies by only roughly a factor of 2.

One possible explanation for the decrease in critical cur-

rent and increase in df/dI is that the effective contact area is altered by the anneals so that a constant current would not correspond to a constant current density. In Fig. 2(a), we plot the device resistance as a function of anneal time. The as-prepared device has a resistance of roughly 8Ω and $I_c = 6.75$ mA. Over the first three anneals the critical current is reduced by a factor of 3 to a value of 2.25 mA.¹⁴ Assuming that the device resistance is inversely proportional to contact area, a corresponding factor of three increase in the resistance would be required for the different critical currents to correspond to a constant current density. However, the device resistance changes by less than 15%, indicating that the contact dimensions are not altered enough to account for the factor of 3 decrease in I_c , although slight changes in the device size, might play some role. Similarly, a change in contact diameter of roughly a factor of 3 would be required to account for the factor of 6 increase in df/dI based on contact size effects.^{15,16} Together, these measurements indicate that changes in the spin-dependent transport in the contact that occur during the first 3 h of annealing are more likely responsible for the initial changes in the oscillator characteristics.

Another possible explanation for the decrease in I_c with thermal anneal is that the magnetic properties of the CoFeB are altered in such a way as to increase the strength of the spin torque effect for a given current density. For instance, within the macrospin approximation, the critical current generally scales as $I_c \propto (\alpha M_s M_{\text{eff}} / \epsilon)$, where α is the Gilbert damping parameter, M_s is the saturation magnetization, M_{eff} is the effective saturation magnetization which includes the out of plane anisotropy, and ϵ is the spin transfer efficiency.¹⁷ Through vector network analyzer based ferromagnetic resonance measurements¹⁸ of identically prepared spin-valve structures, we have found that $\alpha = 0.009 \pm 0.002$, $\mu_0 M_{\text{eff}} = 1.16 \pm 0.05$, and $\mu_0 M_s = 1.44 \pm 0.04$ throughout the anneal process. This is somewhat different from what was measured in Ref. 18 but here, the CoFeB film is grown on a Cu seed layer instead of SiO_2 and the anneals are performed at a lower temperature, which likely accounts for the discrepancies. Within the macrospin approximation, these variations are insufficient to produce the reduced critical currents and observed changes in df/dI . This again indicates that changes in the spin-dependent transport are responsible for the changes in the oscillator behavior during the first several anneals, and that the changes that occur during the later anneals do not result from differences in the magnetostatic properties of the CoFeB film.

The macrospin model is only an approximation to the nanocontact geometry, as there is spinwave radiation away from the contact area. Theoretical models of the nanocontact geometry generally include a second term in the predicted critical current that is proportional to D , the spinwave exchange stiffness, which accounts for this radiation.^{17,19} While this term changes the exact functional form for the critical current, the scaling arguments above are still applicable. Indeed, when a spinwave radiation term is included in the form for the critical current, even greater changes in the device dimensions and material properties are required if they are to properly account for the measured changes in the device

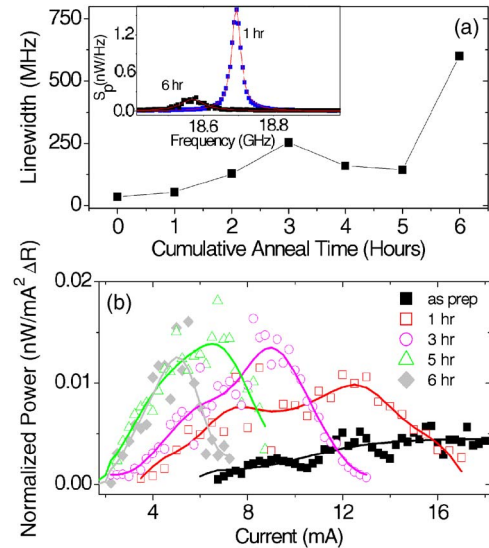


FIG. 3. (Color online) (a) Average linewidths for the data in Fig. 1(a) as a function of cumulative anneal time. (inset) Representative spectral traces for anneal times of 1 and 6 h showing the spectral traces corresponding to the maximum device output power for both anneals. (b) Normalized output power as a function of bias current for several representative anneal times. The solid lines are spline fits to the data and are added only for visual clarity.

characteristics.¹⁴ Hence, the conclusions drawn from the comparison of the data with the macrospin model are justified. We also note that, within the context of current nanocontact theories, the constant value of the critical current during the later anneals precludes the possibility that changes in D can account for the increase in df/dI during the later anneals.

The linewidth, averaged over all current values, is shown in Fig. 3(a) as a function of the cumulative anneal time. In the as-prepared state, the average linewidth is roughly 40 MHz. During the first several anneals, the average linewidth increases and reaches a value of roughly 200 MHz for a cumulative anneal time of 3 h. For anneal times of 4 and 5 h, the average linewidth slightly decreases before increasing by roughly a factor of 4 to 600 MHz at a cumulative anneal time of 6 h, a factor of 15 larger than in the as-prepared device, indicating that the device has degraded. Qualitatively, the overall increase in the average linewidth with annealing mimics the increase in df/dI . However, quantitatively, df/dI increases by roughly a factor of 6 during the anneal process, while the linewidth increases by roughly a factor of 15. This indicates that the linewidths here are not limited by current noise in the system. The measurements were stopped after the sixth anneal as the oscillator linewidths had become quite broad and the absolute output power relatively low [see inset Fig. 3(a)]. This is possibly due to changes in the material microstructure in the vicinity of the contact such as diffusion of CoFe or CoFeB into the Cu layers or a redistribution of B in the free layer. It is also possible that the changes in the spin transfer induced dynamics are due to changes in the material microstructure in the vicinity of the contact, although any such changes would need to be on a level that would not affect the device resistance, and such that they are not reflected in the macroscopic magnetization characteristics. We note that the changes with

annealing have been observed in all contacts measured, and the data are not simply reflecting anomalous changes in the microstructure of a specific device.

The output power, normalized by $I^2\Delta R$, as a function of current is shown in Fig. 3(b). If the precessional trajectories for the various anneal times were nearly identical, then the normalized output power, which accounts for differences in the GMR and bias currents, should also be very similar between the different anneals. However, as seen in Fig. 3(b), this normalization process does not give good agreement between the different anneals, indicating that the mode structure of the oscillations is changing. This can also be seen by comparing the data for the different anneal times shown in Fig. 1(a). For the longest anneal time, the maximum excited frequency is roughly 27 GHz, whereas the maximum frequency is less than 20 GHz in the as-prepared state. As the magnetic properties of the CoFeB film are not changing significantly (the magnetostatic fields within the device are relatively constant), the changes in the excitation frequency are most easily accounted for through changes in the precessional modes of the excitations. The particular changes that are likely occurring are not presently known with certainty. They may correspond to changes in the excitation size, to changes in the mode structure, or may result from changes in the magnitude of the Oersted field. However, we note that, for a given applied field value, the frequency at which the maximum output power occurs is very similar across the anneals (see Fig. 1). While the normalized output powers are not constant throughout the annealing process, this likely indicates that the excited modes are also not too different.

SUMMARY

In summary, we have measured the spectral properties of STNOs with CoFeB as the free layer as a function of successive 225 °C temperature anneals. The anneals result in changes in the oscillator critical current, output power, frequency variation with bias, and oscillator linewidth. The changes that occur during the first several anneals correlate with increases in the GMR of the structure. The later changes likely result from changes in the details of the mode excited by the spin transfer effect. These measurements demonstrate a method of reducing the critical current values in STNOs as

well as increasing their frequency tunability as a function of current as compared to more typical NiFe based devices. They also show the importance of thermal history in CoFeB based devices.

ACKNOWLEDGMENTS

This paper is a contribution of NIST, not subject to copyright.

- ¹M. R. Pufall, W. H. Rippard, and T. J. Silva, *Appl. Phys. Lett.* **83**, 323 (2003).
- ²For a review, see M. D. Stiles and J. Miltat, *Spin Dynamics in Confined Magnetic Structures*, edited by B. Hillebrands and A. Thiaville (Springer, Berlin, 2006), Vol. 3.
- ³S. I. Kiselev, J. C. Sankey, I. N. Krivorotov, N. C. Emley, R. J. Schoelkopf, R. A. Buhrman, and D. C. Ralph, *Nature (London)* **425**, 308 (2003).
- ⁴W. H. Rippard, M. R. Pufall, S. Kaka, S. E. Russek, and T. J. Silva, *Phys. Rev. Lett.* **92**, 027201 (2004).
- ⁵K. Yagami, A. Tulapurkar, A. Fukushima, and Y. Suzuki, *Appl. Phys. Lett.* **85**, 5634 (2004).
- ⁶T. Dimopoulos, G. Gieres, J. Wecker, N. Wiese, and M. Sacher, *J. Appl. Phys.* **96**, 6382 (2004).
- ⁷W. H. Rippard, M. R. Pufall, and S. E. Russek, *Phys. Rev. B* **74**, 224409 (2006).
- ⁸E. B. Myers, F. J. Albert, J. C. Sankey, E. Bonet, R. A. Buhrman, and D. C. Ralph, *Phys. Rev. Lett.* **89**, 196801 (2002).
- ⁹I. N. Krivorotov, N. C. Emley, A. G. F. Garcia, J. C. Sankey, S. I. Kiselev, D. C. Ralph, and R. A. Buhrman, *Phys. Rev. Lett.* **93**, 166603 (2004).
- ¹⁰M. Jimbo, K. Komiyama, Y. Shirota, Y. Fujiwara, S. Tsunashima, and M. Matsuura, *J. Magn. Magn. Mater.* **165**, 308 (1997).
- ¹¹T. Feng and J. R. Childress, *J. Appl. Phys.* **85**, 4937 (1999).
- ¹²We note that the absolute values of the GMR are low due to the relatively thick Cu layers included in the device structure.
- ¹³A. Manchon, N. Strelkov, A. Deac, A. Vedyayev, and B. Dieny, *Phys. Rev. B* **73**, 184418 (2006).
- ¹⁴We note that this method of determining I_c is only approximate since it is limited to measuring the lowest current at which the oscillator power exceeds the noise floor of the measurement. Since the output power is changing with annealing, this makes the reported relative values of I_c as a function of annealing only approximate.
- ¹⁵M. A. Hoefer, M. J. Ablowitz, B. Ilan, M. R. Pufall, and T. J. Silva, *Phys. Rev. Lett.* **95**, 267206 (2005); M. A. Hoefer, Ph.D. thesis, University of Colorado, 2005.
- ¹⁶F. B. Mancoff, N. D. Rizzo, B. N. Engel, and S. Tehrani, *Appl. Phys. Lett.* **88**, 112507 (2006).
- ¹⁷J. C. Slonczewski, *J. Magn. Magn. Mater.* **159**, L1 (1996); **195**, L261 (1999).
- ¹⁸C. Bilzer, T. Devolder, J.-V. Kim, G. Council, C. Chappert, S. Cardoso, and P. Freitas, *J. Appl. Phys.* **100**, 053903 (2006).
- ¹⁹A. N. Slavin and P. Kabos, *IEEE Trans. Magn.* **41**, 1264 (2006).